Journal de Ciencia e Ingeniería, vol.15, no.2, pp.1-14, 2023
http://jci.uniautonoma.edu.co
DOI: https://doi.org/10.46571/JCI.2023.2.1

Corporación Universitaria Autónoma del Cauca
ISSN 2145-2628, e-ISSN 2539-066X
Chemistry

DFT Study and Topological Analysis of the Electron Density of the Casearvestrin

Estudio DFT y Análisis topológico de la densidad electrónica de la Casearvestrina

Michael Zambrano-Angulo[+1], Sol M. Mejía[*2] and Elkin A. Tilvez[+3]
[+]Programa de Química, Facultad de Ciencias Básicas Universidad de la Amazonia-Florencia-Caquetá, Colombia
[*]Departamento de Química, Facultad de Ciencias, Pontificia Universidad Javeriana, Bogotá, Colombia

Abstract. Casearvestrin A, B, and C secundary metabolites, with a promising anticancer potential, were computationally characterized to reveal susceptible sites to nucleophilic and electrophilic attacks, establishing the types and strength of chemical bonds and non-covalent interactions using the B3LYP/6-311++G(d,p) theory level. The chemical behavior prediction was performed by the analysis of local besides global reactivity indexes based on the analysis of the Fukui functions and the topological analysis of the electronic density according to Bader's theory. Casearvestrin A is the most reactive molecule since it has less hardness, smallest band gap, a highest number of C−H−−O weak interactions, and both type of susceptible sites, nucleophilic and electrophilic. Electrophilic attacks are most favored at oxygen atoms of the carbonyl groups, the hydroxyl group, and the cyclic ether. The length of the R chain, which differentiates this type of metabolites, is related to the number of H−−H interactions, which in turn has a relationship with the dipole moment.
Keywords. DFT; Casearvestrin; local and global reactivity indexes; Fukui Function; Quantum Theory of Atoms in Molecules (QTAIM).

Resumen. Las Casearvestrinas A, B, y C son metabolitos secundarios con un gran potencial anticancerígeno, se caracterizaron computacionalmente para revelar los sitios susceptibles a ataques nucleofílicos y electrofílicos, estableciendo los tipos y la naturaleza de los enlaces químicos e interacciones no covalentes utilizando al nivel de teória B3LYP/6-311++G(d,p). La predicción del comportamiento químico se realizó mediante el análisis de índices de reactividad locales además de globales basados en el análisis de las funciones de Fukui y el análisis topológico de la densidad electrónica según la teoría de Bader. El metabolito casearvestrina A mostró ser la molécula más reactiva ya que presenta menor dureza, menor ancho de banda, mayor número de interacciones débiles C−H−−O y ambos tipos de sitios susceptibles, nucleofílico y electrófilo. Los ataques electrofílicos se ven más favorecidos en los átomos de oxígeno de los grupos carbonilo, el grupo hidroxilo y el éter cíclico. La longitud de la cadena R, que diferencia a este tipo de metabolitos, está relacionada con el número de interacciones H—H, que a su vez tiene relación con el momento dipolar .

[1] *e-mail: m.zambrano@udla.edu.co*
[2] *e-mail: sol.mejia@javeriana.edu.co*
[3] *e-mail: e.tilvez@udla.edu.co*

Palabras Claves. DFT; Casearvestrina; Índices de reactividad local y global; Función de fukui; Teoría Cuántica de átomos en moléculas (QTAIM).

How to cite. M. Zambrano, Sol M. Mejía, E. Tílvez, DFT Study and Topological Analysis of the Electron Density of the Casearvestrin. *Jou. Cie. Ing.*, vol. 15, no. 2, pp. 1-14, 2023. doi:10.46571/JCI.2023.2.1

Received: 24/05/2023 **Revised:** 03/08/2023 **Accepted:** 10/11/2023

1. Introduction

In recent decades, research involving plants with medicinal purposes has attracted interest for their possible applications [1–3]. There are various cancer treatments, which depend on their type, location, and state. Among the essential treatments are chemotherapy, radiotherapy, immunotherapy, and gene therapy [4]. Currently, there are no effective treatments since the used drugs cause numerous side effects, and these are usually lengthy and costly. The preparation of new anticancer chemical compounds obtained from natural extracts has become a strategic alternative to curative and palliative treatments for cancer.

Broad plant spices such as *Jacarandacopaia*, *Tapiriraguianensis*, *Gnetumnodiflorum*, *Protiumunifoliolatum*, *Protiumheptaphyllum*, *Costusscaber*, *Crotoncuneatus*, and *Casearia sylvestris* have presented activity against some cancer cell lines [5]. Of particular interest are those plant species for which there have been possible isolations and structure elucidation. This is the case of Casearvestrin A, B, and C as metabolites isolated from Casearia Sylvestris; which were tested in tumor cell lines of the lung, colon, and ovary showing a promissory anticancer potential [6, 7]. The chemical structure of the three secondary metabolites mentioned above was experimentally reported. However, their chemical characteristics are still unknown, although this is of great importance to understand their chemical reactivity. This lack of information could be because experimental assays to reveal the chemical properties of secondary metabolites, in some cases, involve long-term studies that increase the research costs.

However, theoretical chemistry and computational methods can provide methodologies to determine the molecular parameters, such as geometries, electronic structure, polarizabilities, and global and local reactivity indexes to correlate with the available experimental results and, even more, to contribute with some interesting predictions [8–10]. Thus, experimental and theoretical studies reported the importance of the electronic and molecular characterization of many clinically used drugs for disease treatments. For example, Sebastian et al., reported that the reactive sites of 5-chloro-N-(3-nitrophenyl)pyrazine-2-carboxamide are oxygen atoms (electrophilic regions), NH group and nitrogen atoms (nucleophilic regions) through various analyses such as the molecular electrostatic potential, Fukui functions, Natural bond orbital, among others [11]. Besides, other authors have focused on the topological analysis of electron density in order to characterize the nature of the intermolecular and intramolecular interactions, which are essential to understand the reactivity of drugs that present potential cytotoxicity activity [12–15].

Conversely, to our best knowledge, there has not been reported information about the chemical reactivity of Casearvestrin A, B, and C metabolites. Therefore, this investigation reveals the suitable sites for nucleophilic and electrophilic attacks and discovers the action modes of these metabolites at the intermolecular and intramolecular levels employing DFT methods. The analyzes involve local and global reactivity indexes besides topological parameters of the electron density. This kind of research is crucial since it contributes to the first step for computer-aided drug design because it can help find sites of chemical interest and selectively against possible target enzymes.

2. Computational methods

The conformational study of the three secondary metabolites was carried out by calculating the potential energy surface (PES) for each structure using the semi-empirical method PM3 [16] as implemented in the Gaussian 09 molecular modeling software [17]. PM3 offers low computational cost for an initial screening, exploring the PES through the relaxed scan functionality considering the dihedral angles that can form between atoms of the side chain of Casearvestrin metabolites (atoms C_{59}, O_{64}, C_{65}, O_{66}, C_{67}, C_{70}, C_{73}, C_{76}, and C_{79}) (see Figures 1-3). This dihedral angle was varied in steps of 10°, and at each step, the angle was fixed, and the remaining portion of the molecule was optimized. Subsequently, full geometry optimizations and frequency calculations of the most stable conformers of Casearvestrin A, B, and C were performed with Schlegel´s algorithm at B3LYP/6-311++G(d,p) level of theory [18–21]. The energy of the frontier molecular orbitals (the highest occupied molecular orbital, HOMO, and the lowest unoccupied molecular orbital, LUMO) was the base for calculating the global reactivity indexes. According to the Koopmans´ theorem, the ionization potential (I), is the negative of the HOMO energy, while the electron affinity (A), is the negative of the LUMO energy [22]. The global reactivity indexes for the Casearvestrin molecules were determined as follows [23–25]:

$$\Delta\epsilon = (A - I) \qquad (band\ gap) \tag{1}$$

$$\mu = \frac{(A - I)}{2} \qquad (chemical\ potential) \tag{2}$$

$$\eta = \frac{(I - A)}{2} \qquad (chemical\ hardness) \tag{3}$$

$$\sigma = \frac{1}{2\eta} \qquad (chemical\ softness) \tag{4}$$

$$\varpi = \frac{\mu^2}{2\eta} \qquad (electrophilicity) \tag{5}$$

Other reactivity descriptors were the calculation of acceptor chemical potential (μ^+), donor chemical potential (μ^-) electrodonating power (ϖ^-), and electroaccepting power (ϖ^+), which are given by Equations 6-9 [26, 27]:

$$\mu^+ = \frac{1}{4}(I + 3A) \tag{6}$$

$$\mu^- = \frac{1}{4}(2I + A) \tag{7}$$

$$\varpi^+ = \frac{(I + 3A)^2}{16(I + A)} \tag{8}$$

$$\varpi^- = \frac{(3I + 3A)^2}{16(I + A)} \tag{9}$$

Furthermore, the global reactivity indexes for the neutral and ionic systems were calculated by the vertical transition, being the energy of the neutral, anionic, and cationic molecules E, E^- and E^+, respectively. Therefore, the ionization potential and the electron affinity were determined, as shown in Equations 10 and 11

$$I = (E^+ - E) \tag{10}$$

$$A = (E^{-} - E) \tag{11}$$

In order to better evaluate the reactivity of the three Casearvestrin metabolites and reveal the suitable sites for the nucleophilic and electrophilic attacks [28], we calculated the Fukui indexes with respect to x atom, $f_x^{\alpha}(\alpha = +, -)$. Multiplication of the condensed values for global softness gives two expressions for local softness

$$s_x^{+} = S \cdot f_x^{+} \tag{12}$$

$$s_x^{-} = S \cdot f_x^{-} \tag{13}$$

where $f_x^{+} = q_x(N+1) - q_x(N)$ and $f_x^{-} = q_x(N) - q_x(N-1)$ and $q_x(i)$ with $i = N, N-1$, or $N+1$ denotes the electron population of the x atom in the molecule with i electrons.

Finally, a topological analysis was done based on the bond critical points (BCP) and some topological parameters of the electron density evaluated at those BCP, according to Bader´s theory (Quantum Theory of Atoms In Molecules) as implemented at the AIMALL Professional package [29]. A description of the topological parameters employed in this study is reported in the Supplementary Information (SI).

3. RESULTS AND DISCUSSION

3.1. Conformational analysis

An exhaustive conformational analysis was performed through relaxed PES explorations considering dihedral angle rotation. For example, the most stable conformer of Casearvestrin A is shown in Figure 1, besides the two conformers, which correspond to the two maxima of the curve. There is evidence of a substantial increase in energy at the first maximum compared to the second maximum because the oxygen atom (O_{66}) interacts much closer with the hydrogen atom (H_{60}), which generates a repulsion that destabilizes the molecule.

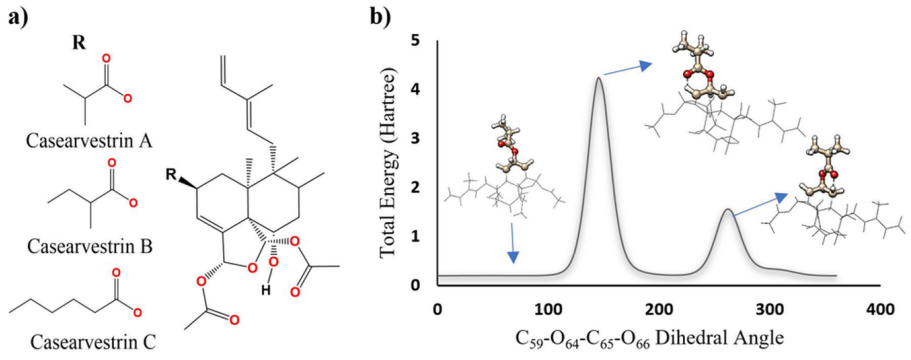

Figure 1: a) General scheme of the molecular structure of the three Casearvestrins. b) Conformational analysis of the Casearvestrin A. Relaxed scan (PM3 method).

Two more PES curves were built by scan calculations because three different dihedral angles were considered for Casearvestrin A, which are C_{59}-O_{64}-C_{65}-O_{66} (see Figure 1), C_{47}-O_{49}-C_{50}-O_{51} and C_{37}-O_{39}-C_{40}-O_{41}, rotating only one dihedral angle at each scan. The same methodology was employed for the conformational analysis of the Casearvestrin B and C. After the conformational

analysis with the PM3 method, the optimized geometries at DFT method of the most stable molecular structures of Casearvestrin A, B, and C were obtained (see Figure 2).

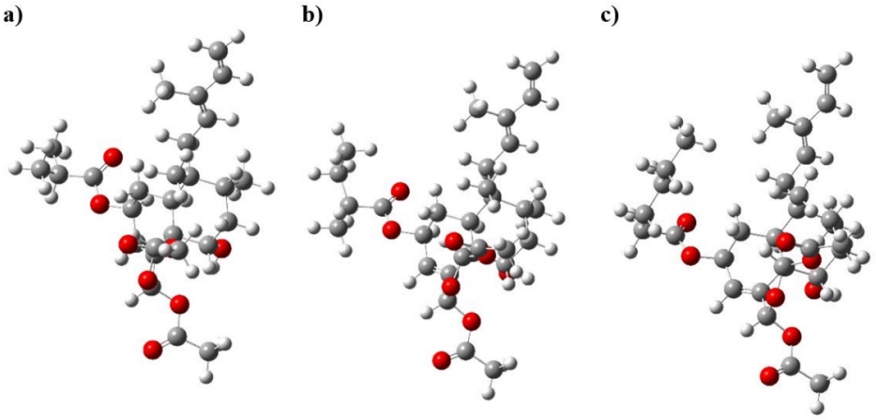

Figure 2: a)Optimized geometries of Casearvestrin metabolites. Casearvestrin A (a), Casearvestrin B (b), and Casearvestrin C (c).

3.2. Global chemical reactivity

Looking to understand how the R chain length can affect the reactivity of the Casearvestrin, the first approach was to calculate the molecular dipole moment finding that a longer R chain (see Figures 1 - 2) confers a higher dipolar moment; Casearvestrin A: 1.3232 Debye, Casearvestrin B: 3.5803 Debye, and Casearvestrin C: 3.5846 Debye. Besides, twelve global reactivity indexes are gathered in Table 1. A system with a high band gap will be a chemically harder system, while a system with a lower band gap will be a softer molecule that is more reactive [9]. In this order of ideas, it is predicted by the Koopmans' theorem values that the most reactive molecule will be Casearvestrin A. Note that the vertical transitions approach does not follow the same hardness order that the Koopmans' theorem values. Besides, global values of donor capacity ϖ^- are much higher than those values of the acceptor capacity ϖ^+ showing close values by both methods used; therefore, the metabolites of Casearvestrin tend much more to donate electrons than to accept them. However, it is prudent to clarify that these behaviors will depend on the medium in which the molecule is found and the systems with which it interacts.

3.3. Local chemical reactivity

To determine which regions are responsible for the different chemical behavior, individual local reactivity was also analyzed. Then, a complete atom label set is displayed in Figure 3 for the three Casearvestrins locating the differences at the R chain.

3.3.1. Molecular electrostatic potentials

To predict the chemical reactivity against nucleophiles and electrophiles, the molecular electrostatic potentials are useful. For example, Zülfikaroğlu et al. have predicted the chemical reactivity of a new hydrazone oxime compound, finding that the most preferred region for an electrophilic attack is around the oxygen atom of the carbonyl group [30]. By contrast, the site of the oxime hydrogen atom is probably involved in nucleophilic processes. According to the

Table 1: Global reactivity indexes for Casearvestrin A, B, and C molecular structures

Method	HOMO	LUMO	ε	μ	χ	η	σ	ω	μ^+	μ^-	ϖ^+	ϖ^-
Casearvestrin A												
Koopman	-143.81	-23.21	120.60	-83.51	83.51	60.30	3265.05	57.82	-53.36	-113.66	23.61	107.11
Vertical	-181.76	-3.33	178.43	-92.54	92.54	89.21	2206.88	48.00	-47.94	-137.15	12.88	105.42
Casearvestrin B												
Koopman	-144.65	-22.68	121.98	-83.67	83.67	60.99	3228.26	57.39	-53.17	-114.16	23.18	106.84
Vertical	-181.89	-4.72	177.17	-93.31	93.31	88.58	2222.58	49.14	-49.02	-137.60	13.56	106.87
Casearvestrin C												
Koopman	-145.01	-23.06	121.95	-84.04	84.04	60.98	3228.93	57.91	-53.55	-114.52	23.51	107.55
Vertical	-181.99	-4.54	177.45	-93.26	93.26	88.73	2219.02	49.02	-48.90	-137.62	13.47	106.74

HOMO (highest occupied molecular orbital), LUMO (lowest unoccupied molecular orbital), ε; Band gap energy, μ; chemical potential, χ; electronegativity, η; hardness, σ; softness, ω; electrophilicity index, μ^+; acceptor potential, μ^-; donor potential, ϖ^+; acceptor capacity y ϖ^-; donor capacity. Row Koopman indicates the use of the Koopmans' theorem to calculate the ionization potential (I) and the electronic affinity (A). In row Vertical, the I and A are calculated as the difference in the total electronic energy between the neutral molecule and the cationic molecule and the difference between the neutral and anionic molecules, respectively. The parameters in this table are defined in the methodology section. All the values in kcal/mol.

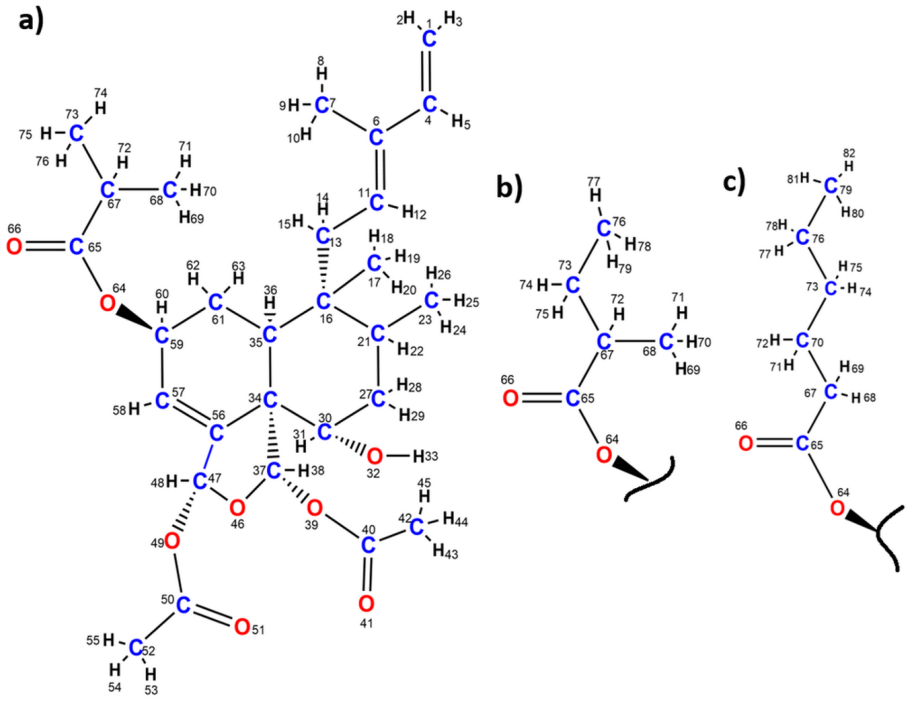

Figure 3: Molecular structures of Casearvestrin A (a), and R chain of Casearvestrin B (b), and Casearvestrin C (c) with atom labels.

color range employed (Figure. 4), the red and yellow areas are mostly related to electrophilic attacks, and the areas with positive potential (blue color) are related to nucleophilic attacks. This is the same color meaning as employed by Sagdinc et al. when analyzing the imipramine hydrochloride molecule as the prototypic tricyclic antidepressant inhibitor of norepinephrine and serotonin neuronal reuptake [31]. For Casearvestrin A, the oxygen atoms 46, 32, 41, 66, and

51 are the most susceptible to receiving an electrophilic attack followed by carbon atoms 11, 6, 4, and 1. This is the oxygen atoms of the carbonyl groups, the hydroxyl group, and the cyclic ether besides the carbon atoms of the double bonds. On the other hand, hydrogen atoms 43, 44, 45, 53, 54, and 33 are the atoms that support the most positive potential, and those atoms are the most reactive in front of a nucleophilic attack. That is hydrogen atoms of the methyl group of the ester functional groups and the hydrogen of the hydroxyl group. Similar trends are shown by Casearvestrin B and C about the oxygen atoms, but the blue region is concentrated mainly on the hydrogen of the hydroxyl group (see Figures 4b and 4c).

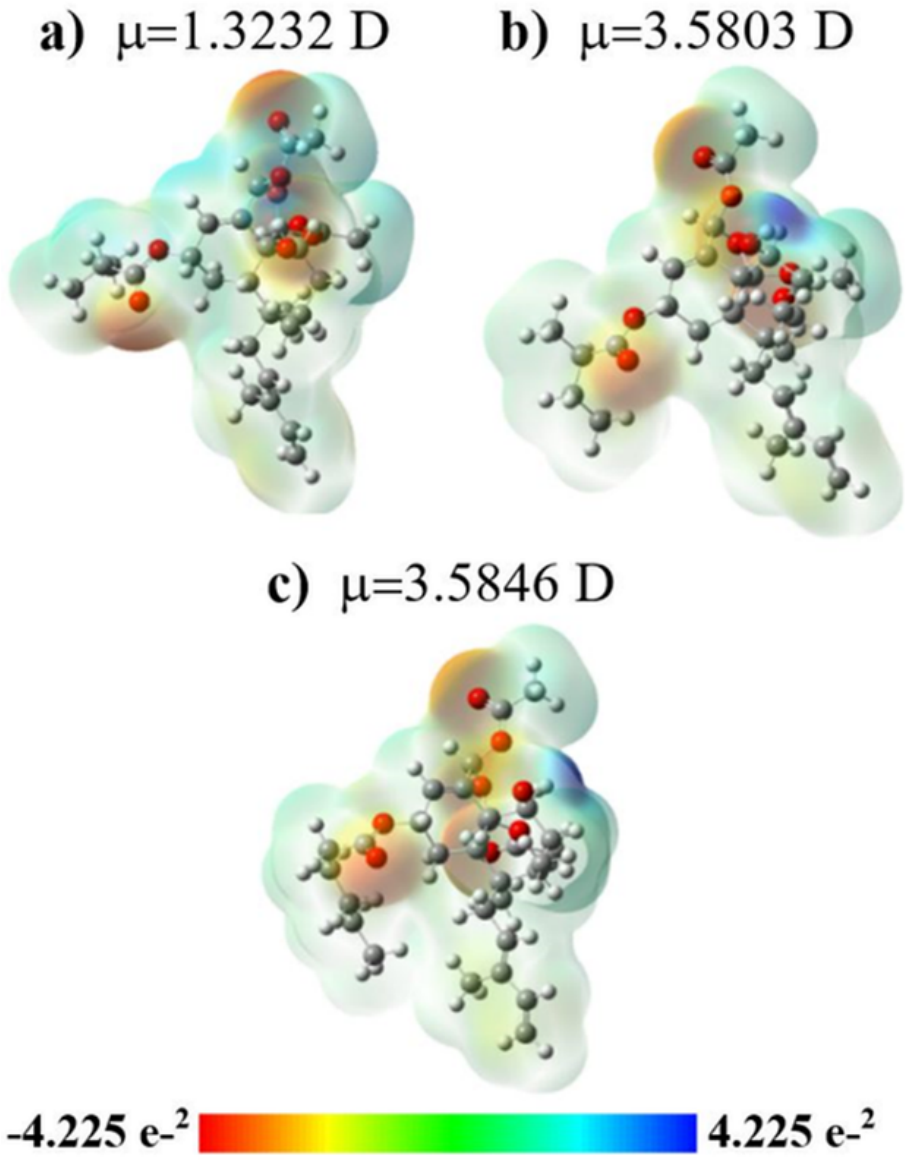

Figure 4: Electrostatic potential maps and the net dipole moment of the a) Casearvestrin A, b) Casearvestrin B, and c) Casearvestrin C molecular structures.

3.3.2. Molecular graphs and topological parameters

The molecular graph on a contour map of the Laplacian of the electron density of the Casearvestrin A is displayed in Figure 5 and that graphic for Casearvestrin B, and C in Figure. 1S at the SI, respectively. Molecular graphs are evidence of the two kinds of weak interactions formation in the three Casearvestrins. Blue dotted lines represent H—H interactions, and red-blue dotted lines represent C-H—O hydrogen bonds. Subsequently, some topological parameters calculated at the bond critical points (BCP) of those weak interactions are gathered in Table 2.

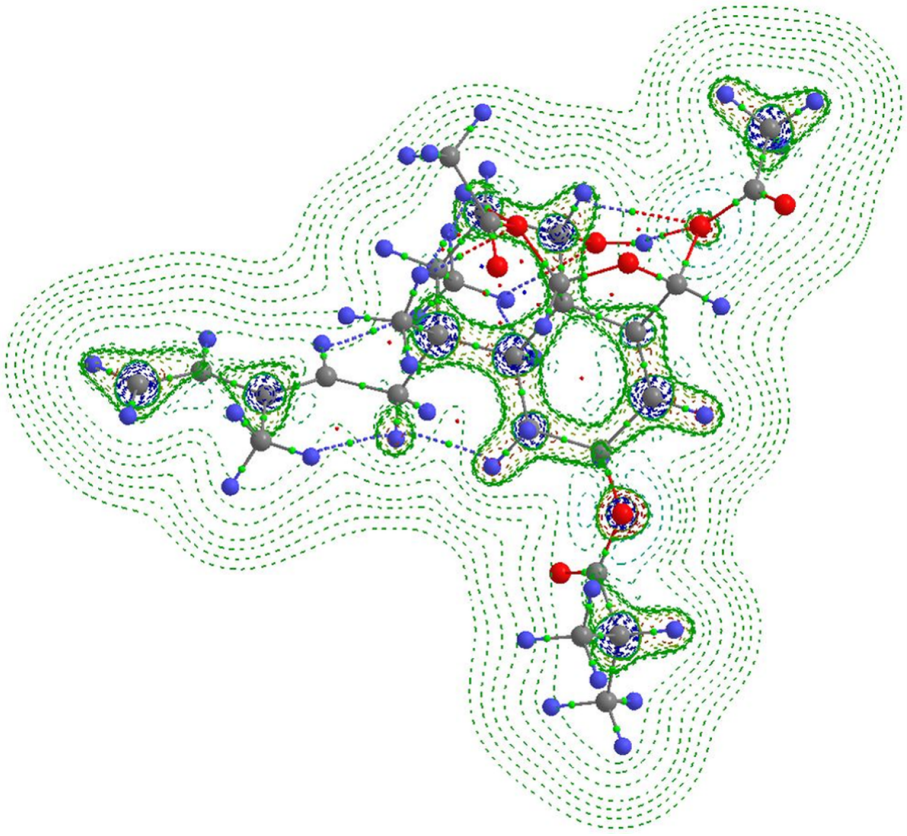

Figure 5: Molecular graph of Casearvestrin A on its contour map of the Laplacian of the electron density. Dotted lines represent the bond path of the weak interactions: blue dotted lines represent H—H interactions, and red-blue dotted lines represent C-H—O hydrogen bonds. Red spheres: oxygen atoms, grey spheres: carbon atoms and blue spheres: hydrogen atoms.

In the current case for H−−H and C−H−−O interactions, the values of $\rho(r_b)$ are less than 0.1 a.u and the values of $\nabla^2\rho(r_b)$ are positive, which is characteristic for these kinds of weak interactions (see a brief description of the topological parameters from QTAIM at the SI). Small differences are observed for both kinds of interactions being a little stronger the C−H−−O. According to the values obtained for the ellipticity, delocalization index, and the total energy density, it can be inferred that both kinds of interactions are very weak and can be broken with any disturbance of the chemical environment. Moreover, there is no direct correlation between the length of the R chain and the abundance of total intermolecular interactions because in Casearvestrin A, there are ten weak interactions, but in Casearvestrin B with longer R chain, there are only eight interactions. However, Casearvestrin A presents one more C−H−−O

Table 2: Topological parameters evaluated at the BCPs for Casearvestrin A, B, and C molecular structures.

Interaction	[a]#Int	[b]$\rho(r_b)$	[c]$\nabla^2\rho(r_b)$	[d]$\varepsilon(r_b)$	[e]DI	[f]$\frac{\lvert\lambda_1\rvert}{\lambda_3}$	[g]$H(r_b)$
Casearvestrin A							
H−−H	5	0.0120	0.0458	0.993	0.023	0.176	0.0022
C−H−−O	5	0.0140	0.0468	0.091	0.038	0.185	0.0007
Casearvestrin B							
H−−H	5	0.0120	0.0470	0.543	0.0248	0.1790	0.0022
C−H−−O	5	0.0140	0.0493	0.104	0.0433	0.1868	0.0008
Casearvestrin C							
H−−H	5	0.0099	0.033	0.354	0.0196	0.175	0.0017
C−H−−O	5	0.0140	0.049	0.102	0.043	0.187	0.0008

[a]#Int: Number of interactions, [b]$\rho(r_b)$: electronic density (Bohr^{-3}),[c] $\nabla^2\rho(r_b)$: Laplacian of electron density (Bohr^{-5}),[d] $\varepsilon(r_b)$: ellipticity (degrees), [e]DI: delocalization index (shared electrons), [f] $\frac{\lvert\lambda_1\rvert}{\lambda_3}$: Relationship between the absolute value of the magnitude of the negative curvature (λ_1) and the positive curvature (λ_3), [g]$H(r_b)$: density of the total energy (Bohr^{-3}*hartree).

interactions in comparison with the other two conformers, which could indicate one of the characteristics that provide most likely and significant sites for its reactivity and could help us to understand why this metabolite is the most reactive of the series.

On the other hand, topological parameters calculated at BCPs of certain chemical bonds indicating each functional group for Casearvestrin A, B and C are shown in Table 3. Other important critical points are shown in Tables S1, S2 and S3 of the SI.

The electronic density values ($\rho(r_b)$) are higher than 0.2 a.u for all BCPs shown in Table 2, which corroborates that these bonds are strong interactions of a covalent type whose breaking would require a significant amount of energy. The smaller values were observed for the $C_{47}-O_{49}$ and $C_{59}-O_{64}$ ester bonds and $C_{37}-O_{46}$ bond with the oxygen located in the Tetrahydrofuran. On the other hand, the highest values correspond to the $C_{40}-O_{41}$, $C_{50}-O_{51}$, and $C_{65}-O_{66}$ bonds; this is, the carbonyl bonds of the molecule (see Figure 3a). Besides, these carbonyl bonds present the most negative values of the density of the total energy ($H(r_b)$), -0.719, -0.718 and -0.705, respectively, indicating that these bonds have high stability concerning the others in the molecule. However, carbonyl bonds are the only bonds with positive Laplacian values. Then, these positive values could be explained because of the resonance of the C=O (C=O $\longleftrightarrow$ C^+ - O^-), which is also inferred from the $\frac{\lvert\lambda_1\rvert}{\lambda_3}$ values minor than 0.5 for those bonds, explaining the resonance movement.

In contrast, the double bonds: $C_{56}-C_{57}$, C_4-C_1, and $C_{11}-C_6$, have the most negative values of the Laplacian; in other words, these present the most covalent character. This is coherent with the highest values of the DI ranging from 1.662 to 1.777 for the double C=C bonds as expected for being double bonds. The lowest values of the DI are 0.779 and 0.763 for $C_{37}-O_{39}$ and $C_{47}-O_{49}$, respectively. In the case of the double bonds, the high values of the ellipticity (0.378, 0.360 and 0.356) are due to the strong π character of the double bond that means that the decrease of the electron density per unit of length is lower along the direction of the bond and is lower in the absolute value of λ_2. Moreover, as the π character of the bond increases, it will also increase torsional stiffness. The highest values of the ellipticity (after the double C=C

Table 3: Topological parameters at the bond critical points of covalent bonds for Casearvestrin A, B y C.

Atoms	$^{a}\rho(r_b)$	$^{b}\nabla^2\rho(r_b)$	$^{c}\varepsilon(r_b)$	^{d}DI	$^{e}\frac{\lvert\lambda_1\rvert}{\lambda_3}$	$^{f}H(r_b)$
Casearvestrin A						
$C_{64} - O_{66}$	0.412	0.182	0.099	1.243	0.482	-0.705
$C_{65} - O_{64}$	0.297	-0.466	0.021	0.839	0.886	-0.445
$C_{59} - O_{64}$	0.237	-0.412	0.032	0.806	1.023	-0.317
Casearvestrin B						
$C_{64} - O_{66}$	0.411	0.169	0.097	1.232	0.484	-0.703
$C_{65} - O_{64}$	0.298	-0.456	0.019	0.845	0.786	-0.466
$C_{59} - O_{64}$	0.236	-0.409	0.029	0.804	1.022	-0.315
Casearvestrin C						
$C_{64} - O_{66}$	0.413	0.177	0.107	1.246	0.485	-0.707
$C_{65} - O_{64}$	0.297	-0.477	0.023	0.839	0.814	-0.462
$C_{59} - O_{64}$	0.236	-0.407	0.030	0.804	1.018	-0.316

$^{a}\rho(r_b)$: electronic density (Bohr^{-3}), $^{b}\nabla^2\rho(r_b)$: Laplacian of electron density (Bohr^{-5}), $^{c}\varepsilon(r_b)$: ellipticity (degrees), ^{d}DI: delocalization index (shared electrons), $^{e}\frac{\lvert\lambda_1\rvert}{\lambda_3}$: Relationship between the absolute value of the magnitude of the negative curvature (λ_1) and the positive curvature (λ_3), $^{f}H(r_b)$: density of the total energy (Bohr^{-3}∗hartree).

bond) were observed for $C_{47} - O_{46}$, $C_{47} - O_{49}$, $C_{37} - O_{46}$ and $C_{37} - O_{39}$ bonds (0.134, 0.140, 0.151, and 0.169, respectively), indicating a particular accumulation of electronic density in the plane that contains the BCP and is orthogonal to the bond.

Finally, mostly values are more significant than 1.0 for the relationship between the absolute value of the magnitude of the negative curvature (λ_1) and the positive curvature (λ_3) in all BCPs. These values indicate that the accumulation of charge exceeds the reduction of the electronic charge in that point as expected for covalent bonds, in this specific molecule, the highest value was 2.6 found at the BCPs of the double C=C bonds.

Values of the topological parameters of covalent bonds at the Casearvestrin B follow the same trend of the Casearvestrin A. ρ_b greater than 0.4 a.u correspond to the carbonyl bonds, values greater than 0.3 a.u belong to the double bonds and the 0.366 a.u value corresponds to the hydroxyl of the molecule. As for the values of $\nabla^2\rho_b$ again the three carbon-oxygen bonds present positive values for the above-mentioned reason, the hydroxyl bond presents the most negative value of the list, and this means that it has the highest stability. $C_{56} - C_{57}$, $C_4 - C_1$, and $C_{11} - C_6$ bonds show values of $\nabla^2\rho_b$ from -0.997 to -0.949. Likewise, these bonds with a large ρ_b and with very negative values of $\nabla^2\rho_b$ showed high values of ε ranging from 0.356 to 0.384. These results indicate that the double bonds have more significant asymmetry in the accumulation of electronic charge in a normal plane to the bond.

On the other hand, the negative values of $H(r_b)$ in all BCP indicate the existence of charge accumulation, and this, in turn, contributes extensively to the stability of the system. The sites that most offer stability to the system are the carbonyl bonds, the hydroxyl group, and the double C=C bonds present in the molecule. DI values reveal the $C_{56} - C_{57}$, $C_4 - C_1$, and $C_{11} - C_6$ bonds like the one with the mayor number of shared electrons as expected for being double bonds. Finally, the values of the $\frac{\lambda_1}{\lambda_3}$ relationship, show values greater than 2 for

carbon-carbon double bonds, then the majority of the electronic charge accumulation is greater than the loss of the same in the closeness of the BCP (values greater than 1). The trends and their interpretation of the topological parameters for Casearvestrin C are similar to the previous two Casearvestrins. Then, according to the values of $\varepsilon(r_b)$, DI(r_b), $H(r_b)$, and $\frac{|\lambda_1|}{\lambda_3}$, the carbonyl type bonds, the hydroxyl group, and the double bonds are the ones that contribute most to the stability of the system. In the last case, this is mainly due to the π character of the double bonds and the rigidity and torsional resistance of them.

3.3.3. Fukui function and local reactivity indexes

Fukui function and local reactivity indexes calculated from atomic charges were calculated from NBO atomic charges. Those data are gathered in Table 4 for Casearvestrin A and in Tables 3S and 4S for Casearvestrin B and C, respectively.

Initiating with Casearvestrin A, according to the values obtained from Mulliken atomic charges for local softness $S_x^-(vert))$, the sites susceptible to an electrophilic attack are carbons 57, 1, and 65 with values for S_x^- of 870.13, 588.92, and 570.85, respectively. These values are consistent with the topological values and those reddest regions observed in Figure 4a which indicates that these areas are the most basic of the system under study. It is essential to clarify that the other carbons present in Table 4 are also susceptible to an electrophilic attack but to a lesser extent. Regarding the nucleophilic attack, the values for local softness $(S_x^+(vert))$ show carbons 1, 11, 21, and 17 as the most susceptible to this attack with these values ranging from 204.92 to 464.22. The values of the condensed Fukui function show the same tendency for both nucleophilic and electrophilic attacks, as observed for local softness. The carbon atom 1 is susceptible to both attacks; however, the electrophilic attack has a higher value indicating that an electrophilic attack will prevail over a nucleophilic attack. The contrary case occurs with carbon atom 11, which is more likely to undergo a nucleophilic attack than an electrophilic attack.

Table 4S shows the values for local descriptors obtained by both methods for the Casearvestrin B molecule. The condensed local softness (S_x^-) values associated with electrophile attacks show as main susceptible sites carbon atoms 21, 34, and 57 by both methods with values from 976.53 to 4587.06 by the vertical transition method and from 672.32 to 3158.08 using the Koopmans' theorem. The nucleophilic attacks that are associated with the value of condensed softness (S_x^+) reveals that the most susceptible atom to receive an attack of this type is carbon 1 with a condensed softness value of 435.58 (vert) and 299.89 (Koop) followed by the atoms 11 and 4 with values 224.06 and 221.22 (vert), respectively, these atoms form double bonds. Therefore, it can be inferred that the double bonds are sites susceptible to receiving attacks by nucleophiles. The same trend was found for the Fukui function but with lower values.

The Fukui function through the NBO charges for Casearvestrin B predicts as suitable sites for electrophilic attacks $(S_x^-(Vert))$ the atoms of carbon 59 and 7 and hydrogen 78 with values between 22.44 and 27.99. As it can be noticed and like the previous molecule, the values obtained for the NBO charges are smaller compared to those obtained with the Mulliken charges, whereas for the nucleophilic attacks $(S_x^+(Vert))$ show a similar tendency given as the most reactive sites: carbon 1, 11, and 6 with values ranging from 297.0 to 632.29. The Fukui function shows the same trend for both electrophilic and nucleophilic sites as local softness parameters.

The values of softness obtained from Milliken charges $(S_x^-(Vert))$ reveal the carbon atoms 21, and 34 of the Casearvestrin C as the most susceptible to be attacked by electrophiles, with values of 4961.61 and 2513.08, respectively (see Table 4S). On the other hand, the condensed softness (S_x^+) shows as central atoms prone to nucleophilic attacks the carbon atoms 1 and 11, which, like in the previous molecule, which forms double bonds; this condensed softness also states the hydrogen atoms 10, 12 and 3 which are atoms close to the aforementioned carbon atoms with that chemical behavior. Finally, the condensed Fukui function shows the same tendency for both

Table 4: Fukui function and local reactivity indexes (softness) calculated from Mulliken and NBO charges for Casearvestrin A molecular structure.

MULLIKEN							
NUCLEOPHILIC				ELECTROPHILIC			
ATOM (x)	f_x^{+a}	$S_x^{+a}(Vert)^b$	$S_x^{+a}(Koop)^c$	ATOM(x)	f_x^{-a}	$S_x^{-a}(Vert)^b$	$S_x^{-a}(Koop)^c$
C_1	89.22	464.22	313.77	C_{57}	167.23	870.13	588.13
C_{11}	43.17	224.60	151.81	C_1	113.19	588.92	398.06
C_{21}	41.81	217.57	147.06	C_{65}	109.71	570.85	385.85
C_{17}	39.38	204.92	138.51	C_{35}	82.68	430.18	290.76
H_3	37.53	195.27	131.98	C_{50}	68.53	356.56	241.00
H_{12}	34.00	176.89	119.56	C_{68}	46.80	243.50	164.59
H_2	30.81	160.33	108.37	C_{73}	36.27	188.70	127.55
H_5	30.50	158.68	107.26	C_{11}	35.38	184.08	124.42
H_{14}	29.57	153.84	103.98	C_{56}	34.55	179.76	121.50
H_8	23.44	121.96	82.43	C_{23}	30.55	158.96	107.44
NBO							
NUCLEOPHILIC				ELECTROPHILIC			
ATOM(x)	f_x^{+a}	$S_x^{+a}(Vert)^b$	$S_x^{+a}(Koop)^c$	ATOM(x)	f_x^{-a}	$S_x^{-a}(Vert)^b$	$S_x^{-a}(Koop)^c$
C_1	129.40	673.29	455.08	C_{59}	7.96	41.40	27.98
C_{11}	115.89	602.99	407.57	C_{34}	4.89	25.47	17.21
C_6	62.80	326.77	220.86	O_{64}	4.47	23.25	15.71
H_{14}	25.04	130.28	88.05	C_7	3.94	20.50	13.86
C_{57}	22.58	117.48	79.40	C_{27}	1.85	9.63	6.51
H_{10}	18.27	95.08	64.26	H_{75}	1.65	8.59	5.80
O_{32}	18.27	95.05	64.24	C_{42}	1.63	8.49	5.74
H_8	17.78	92.50	62.52	C_{23}	1.56	8.10	5.47
H_3	14.60	75.98	51.35	C_{13}	1.40	7.28	4.92
H_{31}	14.38	74.83	50.58	H_{26}	0.68	3.56	2.41

$f_x^{\pm a}$: condensed Fukui function, ${}^bS_x^{\pm}(Vert)$ and ${}^cS_x^{\pm}(Koop)$: local softness obtained by vertical transitions and Koopmans' theorem, respectively.

attacks, as observed for the softness parameter. The values of the local descriptors obtained by the NBO charges for the Casearvestrin C molecule, as well as the previous molecules, show very low values for the local softness condensed associated with electrophilic attacks (s_x^-). These indicate that hydrogen atoms 80 and 75 are the most susceptible to this type of attack while the condensed softness, which is associated with the nucleophilic attacks (s_x^+), shows the carbon atoms 1 and 11 as the most likely to receive attacks by nucleophiles as the results obtained by the Mulliken charges also reveals. Finally, the Fukui function shows the same tendency for both attacks showing as susceptible atoms the previously named.

4. CONCLUSIONS

The analysis of global reactivity indexes besides local parameters based on the topological analysis of the electronic density according to the Quantum Theory of Atoms In Molecules and the analysis of the Fukui Functions allowed to reveal the types and strengths of intramolecular and intermolecular interactions and the susceptible sites for nucleophilic and electrophilic attacks for Casearvestrin A, B, and C. It is predicted that the most susceptible sites to an electrophilic attack are the oxygen atoms of the carbonyl groups, the hydroxyl group and the cyclic ether

besides the carbon atoms of the double C=C bonds due to their high density and their negative electrostatic potential values no matter the studied metabolite. The nucleophilic attacks can be predicted in the same and correct way using any of the two methods, Mulliken or NBO, while for electrophilic attacks, different trends were obtained for each used method. Casearvestrin A is the most reactive in the series since it is the metabolite with less hardness, smallest band gap, a highest number of C−H−−O interactions and with susceptible sites to different attacks in a chemical reaction showing more preference for electrophilic attacks but that difference is not as big as observed for both sites at Casearvestrin B and C. The R chain length does not affect the covalent character of the rest of the bonds, but a longer R chain more significant molecular dipole moment and a higher number of H−−H interactions.

References

[1] D.J. Newman and G.M. Cragg, "Natural Products as Sources of New Drugs from 1981 to 2014," *Journal of Natural Products*, vol. 79, no. 3, pp. 629-661, 2016.

[2] Q. Zhao et al., "Anticancer effects of plant derived Anacardic acid on human breast cancer MDA-MB-231 cells," *American journal of translational research*, vol. 10, no. 8, pp. 2424-2434, 2018.

[3] R. Sarria-Villa, and J. Gallo-Corredor. "El eucalipto como fuente de materia prima para la extracción de aceites esenciales", *Jou. Cie. Ing.* , vol. 11, no. 1 p. 57-64, 2019.

[4] R. Weissleder and M. J. Pittet, "Imaging in the era of molecular oncology," *Nature*, vol. 452, no. 7187, pp. 580-589, 2008.

[5] M. S. Akhtar and M. K. Swamy, Anticancer Plants: Properties and Application (no. v. 1). Springer, 2018.

[6] N. H. Oberlies et al., "Novel Bioactive Clerodane Diterpenoids from the Leaves and Twigs of Casearia sylvestris", *Journal of Natural Products*, vol. 65, no. 2, pp. 95-99, 2002.

[7] I. Piyanzina, B. Minisini, D. Tayurskii, and J.-F. J. J. o. M. M. Bardeau, "Density functional theory calculations on azobenzene derivatives: a comparative study of functional group effect," *J. Mol Model* 21, p. 34, 2015

[8] I. Piyanzina, B. Minisini, D. Tayurskii, and J.-F. J. J. o. M. M. Bardeau, "Density functional theory calculations on azobenzene derivatives: a comparative study of functional group effect," *J. Mol Model* 21, p. 34, 2015.

[9] S. M. Aguilera-Segura, F. Di Renzo, and T. J. J. o. M. M. Mineva, "Structures, intermolecular interactions, and chemical hardness of binary water–organic solvents: a molecular dynamics study," *J. Mol Model* vol. 24, no. 10, p. 292, 2018.

[10] J.-L. Vigneresse and L. J. J. o. M. M. Truche, "Chemical descriptors for describing physico-chemical properties with applications to geosciences," *journal article* vol. 24, no. 9, p. 231, 2018.

[11] S. H. R. Sebastian et al., "Spectroscopic, quantum chemical studies, Fukui functions, in vitro antiviral activity and molecular docking of 5-chloro-N-(3-nitrophenyl)pyrazine-2-carboxamide," *Journal of Molecular Structure*, vol. 1119, pp. 188-199, 2016.

[12] Y. A. Abramov, "QTAIM Application in Drug Development: Prediction of Relative Stability of Drug Polymorphs from Experimental Crystal Structures," *J. Phys. Chem. A*, vol. 115, no. 45, pp. 12809-12817, 2011.

[13] M. Raja, R. Raj Muhamed, S. Muthu, M. Suresh, and K. Muthu, "Synthesis, spectroscopic (FT-IR, FT-Raman, NMR, UV–Visible), Fukui function, antimicrobial and molecular docking study of (E)-1-(3-bromobenzylidene)semicarbazide by DFT method," *Journal of Molecular Structure*, vol. 1130, pp. 374-384, 2017.

[14] R. D. Tosso et al., "The electronic density obtained from a QTAIM analysis used as molecular descriptor. A study performed in a new series of DHFR inhibitors," *Journal of Molecular Structure*, vol. 1134, pp. 464-474, 2017.

[15] F. J. Melendez et al., "Analysis of the topology of the electron density and the reactivity descriptors of biomolecules with insecticide activity," *Theoretical Chemistry Accounts*, vol. 135, no. 8, p. 206, 2016.

[16] J.P. Stewart, "Optimization of parameters for semiempirical methods I. Method," *Journal of Computational Chemistry*, vol. 10, no. 2, p. 209-220, 1989.

[17] M. Frisch et al., "Gaussian 09, revision a. 02, gaussian," vol. 200, p. 28, 2009

[18] S. H. Vosko, L. Wilk, and M. Nusair, "Accurate spin-dependent electron liquid correlation energies for local spin density calculations: a critical analysis" *Canadian Journal of Physics*, vol. 58, no. 8, p. 1200-1211, 1980.

[19] A. D. Becke, "Density-functional exchange-energy approximation with correct asymptotic behavior", *Physical Review A*, vol. 38, no. 6, p. 3098-3100, 1988.

[20] C. Lee, W. Yang, and R. G. Parr, "Development of the Colle-Salvetti correlation-energy formula into a functional of the electron density" *Physical Review B*, vol. 37, no. 2, p. 785-789, 1988.
[21] C. Gonzalez and H. B. Schlegel, "An improved algorithm for reaction path following", *Chem. Phys.*, vol. 90, no. 4, p. 2154-2161, 1989.
[22] T. Koopmans, "Über die Zuordnung von Wellenfunktionen und Eigenwerten zu den Einzelnen Elektronen Eines Atoms", *Physica*, vol. 1, no. 1, p. 104-113, 1934.
[23] R. G. Parr and R. G. Pearson, "Absolute hardness: companion parameter to absolute electronegativity", *Journal of the American Chemical Society,*, vol. 105, no. 26, p. 7512-7516, 1983.
[24] L. R. Domingo, M. Ríos-Gutiérrez, and P. Pérez, "Applications of the Conceptual Density Functional Theory Indices to Organic Chemistry Reactivity" *molecules*, vol. 21, no. 6, p. 748, 2016.
[25] C.-G. Zhan, J. A. Nichols, and D. A. Dixon, "Ionization Potential, Electron Affinity, Electronegativity, Hardness, and Electron Excitation Energy: Molecular Properties from Density Functional Theory Orbital Energies", *The Journal of Physical Chemistry A*, vol. 107, no. 20, p. 4184-4195, 2003.
[26] J. L. Gázquez, A. Cedillo, and A. Vela, "Electrodonating and Electroaccepting Powers", *The Journal of Physical Chemistry A*, vol. 111, no. 10, p. 1966-1970, 2007.
[27] P. Geerlings, F. De Proft, and W. Langenaeker, "Conceptual Density Functional Theory", *Chemical Reviews*, vol. 103, no. 5, p. 1793-1874, 2003.
[28] P. W. Yang and W. J. Mortier, "The use of global and local molecular parameters for the analysis of the gas-phase basicity of amines". *Journal of the American Chemical Society*, vol. 108, no. 19, p. 5708-5711, 1986.
[29] T. J. O. h. a. t. c. Keith, "AIMAll (Version 15.09. 27); TK Gristmill Software: Overland Park, KS, 2010.
[30] A. Zülfikaroğlu, H. Batı, and N. Dege, "A theoretical and experimental study on isonitrosoacetophenone nicotinoyl hydrazone: Crystal structure, spectroscopic properties, NBO, NPA and NLMO analyses and the investigation of interaction with some transition metals", *Journal of Molecular Structure*, vol. 1162, p. 125-139, 2018.
[31] S. G. Sagdinc, C. Azkeskin, and A. Eşme, "Theoretical and spectroscopic studies of a tricyclic antidepressant, imipramine hydrochloride", *Journal of Molecular Structure* , vol. 1161, p. 169-184, 2018.